

Topologically protected flat zero-energy surface bands in noncentrosymmetric superconductors

P. M. R. Brydon,^{1,*} Andreas P. Schnyder,^{2,†} and Carsten Timm¹

¹*Institut für Theoretische Physik, Technische Universität Dresden, D-01062 Dresden, Germany*

²*Max-Planck-Institut für Festkörperforschung, Heisenbergstrasse 1, D-70569 Stuttgart, Germany*

(Received 15 April 2011; revised manuscript received 27 May 2011; published 6 July 2011)

Nodal noncentrosymmetric superconductors (NCS) have recently been shown to be topologically nontrivial. An important consequence is the existence of topologically protected flat zero-energy surface bands, which are related to the topological characteristics of the line nodes of the bulk gap via a bulk-boundary correspondence [A. P. Schnyder and S. Ryu, [arXiv:1011.1438](https://arxiv.org/abs/1011.1438)]. In this Rapid Communication, we examine these zero-energy surface bands using a quasiclassical theory. We determine their spectrum and derive a general condition for their existence in terms of the sign change of the gap functions. A key experimental signature of the zero-energy surface bands is a zero-bias peak in the tunneling conductance, which depends strongly on the surface orientation. This can be used as a fingerprint of a topologically nontrivial NCS.

DOI: [10.1103/PhysRevB.84.020501](https://doi.org/10.1103/PhysRevB.84.020501)

PACS number(s): 74.50.+r, 03.65.Vf, 74.20.Rp, 74.25.F–

I. INTRODUCTION

A key experimental signature of topological insulators and superconductors is the existence of topologically protected zero-energy surface or edge states, some of which are of Majorana type.^{1–4} But, zero-energy boundary modes of topological origin can also occur in gapless topological systems that exhibit topologically stable Fermi points or in nodal superconductors with nontrivial topology. In such systems, one generically finds topologically protected dispersionless zero-energy surface states, i.e., flat bands at the surface. Such flat bands are known to occur at the zig-zag and bearded edge in graphene,^{5,6} on the (110) surface of a $d_{x^2-y^2}$ -wave superconductor,^{7,8} within vortices in the A phase of ³He,⁹ and in other systems with topologically protected Dirac points.¹⁰

It has recently been realized that nodal noncentrosymmetric superconductors (NCS) are topologically nontrivial states of matter.^{11–13} An NCS is realized in a system lacking inversion symmetry, which gives rise to an antisymmetric spin-orbit (SO) coupling and consequently to the admixture of spin-singlet and spin-triplet components in the superconducting state. There is a steadily growing list of these remarkable materials, most notably $\text{Li}_2\text{PdPt}_{3-x}\text{B}$,^{14,15} Y_2C_3 ,¹⁶ and the heavy-fermion compounds CePt_3Si ,¹⁷ CeRhSi_3 ,¹⁸ and CeIrSi_3 .¹⁹ It is predicted that the topological nontriviality of a nodal NCS leads to topologically protected zero-energy surface bands, which only occur within regions of the surface Brillouin zone bounded by the projected nodal lines of the bulk gap. Since these zero-energy surface bands give a singular contribution to the surface density of states, we can expect them to lead to a zero-bias conductance peak (ZBCP).

It is the aim of this Rapid Communication to investigate the appearance of zero-energy surface bands in an NCS using the quasiclassical scattering theory.⁸ This method is ideal for exploring the bound surface states of unconventional superconductors, and has revealed key aspects of the surface physics of the cuprate high- T_c compounds^{7,8} and NCS systems.^{20–25} We hence derive the surface-bound-state spectrum and a general condition for the existence of the zero-energy surface bands in terms of a sign change of the superconducting gap function across the Fermi surface. This condition is complementary to the topological criterion given in Ref. 13. We then compute

the tunneling conductance between a normal metal and an NCS as a function of both the surface orientation and the relative magnitude of the spin-singlet and spin-triplet pairing states. We argue that the strong dependence of the ZBCP on both these variables provides a powerful diagnostic test of the pairing state of an NCS, while also directly evidencing the topologically protected zero-energy surface bands.

II. MODEL SYSTEM

We phenomenologically model the NCS as a single-band system, described by the Bogoliubov–de Gennes (BdG) Hamiltonian

$$\mathcal{H}(\mathbf{k}) = \begin{pmatrix} \varepsilon(\mathbf{k}) + \mathbf{g}(\mathbf{k}) \cdot \boldsymbol{\sigma} & \Delta(\mathbf{k}) \\ \Delta^\dagger(\mathbf{k}) & -\varepsilon(\mathbf{k}) + \mathbf{g}(\mathbf{k}) \cdot \boldsymbol{\sigma}^* \end{pmatrix}, \quad (1)$$

where $\varepsilon(\mathbf{k})$ is the spin-independent part of the band dispersion, $\mathbf{g}(\mathbf{k}) = -\mathbf{g}(-\mathbf{k})$ is the antisymmetric SO coupling, and $\Delta(\mathbf{k}) = [\Delta_s + \mathbf{d}(\mathbf{k}) \cdot \boldsymbol{\sigma}](i\sigma_y)$ is the superconducting gap function. It is convenient to express the Hamiltonian Eq. (1) in the so-called helicity basis, which diagonalizes the kinetic term, yielding two helicity bands with dispersions $\xi^\pm(\mathbf{k}) = \varepsilon(\mathbf{k}) \pm |\mathbf{g}(\mathbf{k})|$. In the absence of interband pairing, the critical temperature is maximized by taking the spin-triplet pairing vector $\mathbf{d}(\mathbf{k})$ to be aligned with the polarization vector of the SO coupling $\mathbf{g}(\mathbf{k})$,²⁶ i.e., we parametrize the triplet component of the gap function and the SO coupling as $\mathbf{d}(\mathbf{k}) = \Delta_t \mathbf{l}_k$ and $\mathbf{g}(\mathbf{k}) = \alpha \mathbf{l}_k$, respectively. Hence, the gaps on the two helicity bands are $\Delta_k^\pm = \Delta_s \pm \Delta_t |\mathbf{l}_k| = \Delta_0(q \pm |\mathbf{l}_k|)/(q + 1)$, where the parameter $q = \Delta_s/\Delta_t$ interpolates between pure triplet pairing ($q = 0$) and pure singlet pairing ($q \rightarrow \infty$). For simplicity, we assume the pairing amplitudes Δ_s and Δ_t to be constant and have positive sign.²⁷ We note that higher-order angular momentum components of the gap Δ_0 have also been studied.^{22,24,28–30}

The specific form of the pseudovector \mathbf{l}_k depends on the symmetries of the noncentrosymmetric crystal.³¹ Ignoring the periodic Brillouin-zone structure, we employ a small-momentum expansion, which, for the tetragonal point group C_{4v} (relevant for CePt_3Si , CeRhSi_3 , and CeIrSi_3), gives to lowest order the symmetry-allowed form

$$\mathbf{l}_k = k_y \hat{x} - k_x \hat{y}. \quad (2a)$$

For the cubic point group O , which is relevant for $\text{Li}_2\text{Pd}_x\text{Pt}_{3-x}\text{B}$, the expansion of $\mathbf{l}_{\mathbf{k}}$ reads as

$$\mathbf{l}_{\mathbf{k}} = k_x(1 + g_2[k_y^2 + k_z^2])\hat{\mathbf{x}} + k_y(1 + g_2[k_x^2 + k_z^2])\hat{\mathbf{y}} + k_z(1 + g_2[k_x^2 + k_y^2])\hat{\mathbf{z}}. \quad (2b)$$

For the spherical Fermi surfaces considered below, the gap $\Delta_{\mathbf{k}}^-$ only has nodes if $g_2 \neq 0$. Finally, we also consider the tetrahedral point group T_d , experimentally represented by Y_2C_3 , where $\mathbf{l}_{\mathbf{k}}$ takes the form

$$\mathbf{l}_{\mathbf{k}} = k_x(k_y^2 - k_z^2)\hat{\mathbf{x}} + k_y(k_z^2 - k_x^2)\hat{\mathbf{y}} + k_z(k_x^2 - k_y^2)\hat{\mathbf{z}}. \quad (2c)$$

III. SURFACE BOUND STATES

We wish to solve the BdG equation $\hat{H}\Psi(\mathbf{r}) = E\Psi(\mathbf{r})$ at a surface for states that decay into the bulk, i.e., that have energies lying within the gap. We define coordinates parallel (\mathbf{r}_{\parallel}) and perpendicular (r_{\perp}) to the surface such that the NCS occupies the half-space $r_{\perp} > 0$. For simplicity, we ignore the SO splitting of the bands and assume coincident spherical helical Fermi surfaces with radius k_F .^{21,22,25} We have verified that relaxing this approximation does not alter the condition for the existence of zero-energy surface bands. It is therefore convenient to regard the momentum components in the definition of $\mathbf{l}_{\mathbf{k}}$ [Eq. (2)] as normalized by k_F . If we take $g_2 = -1.5$ in Eq. (2b), then, for all point groups, we find that $\Delta_{\mathbf{k}}^-$ has point nodes for $q = 0, 1$, line nodes for $0 < q < 1$, and is fully gapped for $q > 1$. Examples of the nodal structure of $\Delta_{\mathbf{k}}^-$ are shown in Fig. 1.

We obtain the following ansatz for the surface-bound-state wave function:

$$\Psi(\mathbf{k}_{\parallel}, \mathbf{r}) = \sum_{n=\pm} \sum_{\mathbf{p}=\mathbf{k}, \tilde{\mathbf{k}}} a_n(\mathbf{p}) \psi_n(\mathbf{p}) e^{-\kappa_{\mathbf{p}}^{\pm} r_{\perp}} e^{i\mathbf{p}\cdot\mathbf{r}}, \quad (3)$$

where $\mathbf{k} = (\mathbf{k}_{\parallel}, k_{\perp})$ and $\tilde{\mathbf{k}} = (\mathbf{k}_{\parallel}, -k_{\perp})$ are wave vectors with $|\mathbf{k}| = |\tilde{\mathbf{k}}| = k_F$. The momentum component parallel to the surface \mathbf{k}_{\parallel} is a good quantum number due to translational invariance. The positive and negative helicity components $\psi_{\pm}(\mathbf{p})$ are given by

$$\psi_{+}(\mathbf{p}) = \left(1, \frac{l_{\mathbf{p}}^x + il_{\mathbf{p}}^y}{|\mathbf{l}_{\mathbf{p}}| + l_{\mathbf{p}}^z}, -\frac{l_{\mathbf{p}}^x + il_{\mathbf{p}}^y}{|\mathbf{l}_{\mathbf{p}}| + l_{\mathbf{p}}^z} \gamma_{\mathbf{p}}^{+}, \gamma_{\mathbf{p}}^{+} \right)^T, \quad (4a)$$

$$\psi_{-}(\mathbf{p}) = \left(\frac{l_{\mathbf{p}}^x - il_{\mathbf{p}}^y}{|\mathbf{l}_{\mathbf{p}}| + l_{\mathbf{p}}^z}, -1, \gamma_{\mathbf{p}}^{-}, \frac{l_{\mathbf{p}}^x - il_{\mathbf{p}}^y}{|\mathbf{l}_{\mathbf{p}}| + l_{\mathbf{p}}^z} \gamma_{\mathbf{p}}^{-} \right)^T, \quad (4b)$$

respectively, with $\gamma_{\mathbf{p}}^{\pm} = (\Delta_{\mathbf{p}}^{\pm})^{-1} [E - i \text{sgn}(p_{\perp}) (|\Delta_{\mathbf{p}}^{\pm}|^2 - E^2)^{1/2}]$. The wave-function components decay into the bulk over the inverse length scale $\kappa_{\mathbf{p}}^{\pm} = m(\hbar^2 |p_{\perp}|)^{-1} (|\Delta_{\mathbf{p}}^{\pm}|^2 - E^2)^{1/2}$, where m is the effective mass.

A bound state occurs if the coefficients $a_n(\mathbf{p})$ in Eq. (3) can be chosen so that the wave function vanishes at the surface. After some algebra, this yields the following condition for surface-bound-state formation:

$$0 = (\gamma_{\mathbf{k}}^{+} - \gamma_{\mathbf{k}}^{-})(\gamma_{\tilde{\mathbf{k}}}^{-} - \gamma_{\tilde{\mathbf{k}}}^{+})(|\mathbf{l}_{\mathbf{k}}||\mathbf{l}_{\tilde{\mathbf{k}}}| - \mathbf{l}_{\mathbf{k}} \cdot \mathbf{l}_{\tilde{\mathbf{k}}}) + (\gamma_{\mathbf{k}}^{+} - \gamma_{\tilde{\mathbf{k}}}^{+})(\gamma_{\mathbf{k}}^{-} - \gamma_{\tilde{\mathbf{k}}}^{-})(|\mathbf{l}_{\mathbf{k}}||\mathbf{l}_{\tilde{\mathbf{k}}}| + \mathbf{l}_{\mathbf{k}} \cdot \mathbf{l}_{\tilde{\mathbf{k}}}). \quad (5)$$

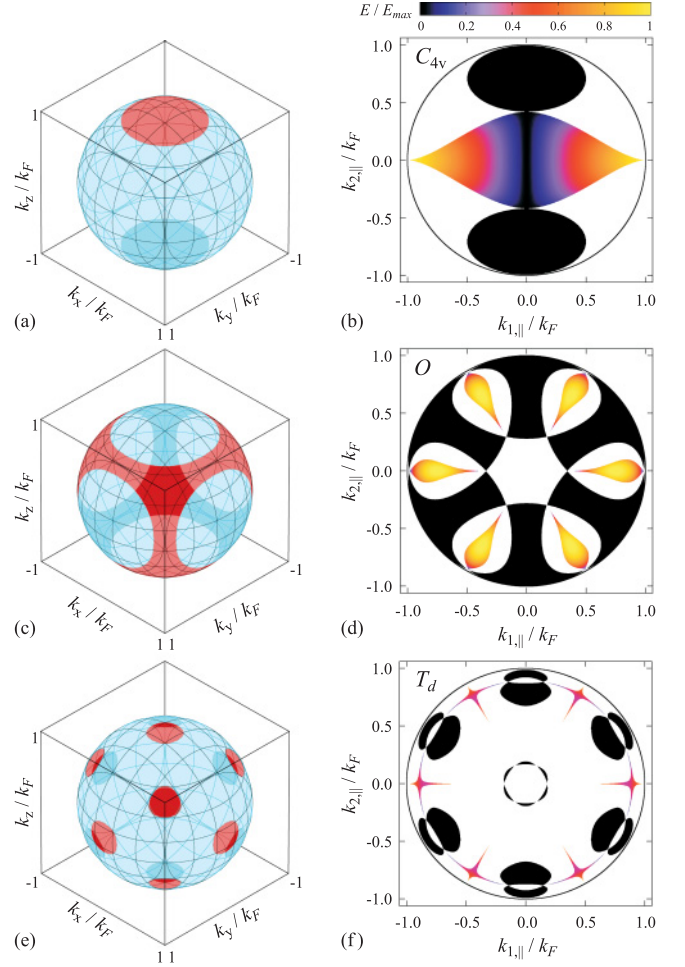


FIG. 1. (Color online) Panels (a), (c) and (e): Variation of the sign of $\Delta_{\mathbf{k}}^-$ over the Fermi surface as seen along the (111) direction for (a) the C_{4v} point group with $q = 0.5$, (c) the O point group with $q = 0.35$, and (e) the T_d point group with $q = 0.4$. Dark red indicates $\text{sgn}(\Delta_{\mathbf{k}}^-) = 1$, whereas light blue is $\text{sgn}(\Delta_{\mathbf{k}}^-) = -1$. Panels (b), (d) and (f): Surface bound states at the (111) face corresponding to the same parameters as in (a), (c) and (e), respectively. The color scale of each plot is normalized by the maximum bound state energy, (b) $E_{\max} = 0.333 \Delta_0$, (d) $E_{\max} = 0.211 \Delta_0$, and (f) $E_{\max} = 0.421 \Delta_0$. White space indicates the absence of a bound state, and the circle is the projection of the Fermi surface, i.e., $|\mathbf{k}_{\parallel}| = k_F$.

Setting $E = 0$ in Eq. (5) and observing that $\gamma_{\mathbf{p}}^{\pm}|_{E=0} = -i \text{sgn}(p_{\perp}) \text{sgn}(\Delta_{\mathbf{p}}^{\pm})$, we find that Eq. (5) has a nontrivial zero-energy solution whenever (i) $\text{sgn}(\Delta_{\mathbf{k}}^-) = \text{sgn}(\Delta_{\tilde{\mathbf{k}}}^-) = -1$ and $\mathbf{l}_{\mathbf{k}} \cdot \mathbf{l}_{\tilde{\mathbf{k}}} = -|\mathbf{l}_{\mathbf{k}}||\mathbf{l}_{\tilde{\mathbf{k}}}|$ or (ii) $\text{sgn}(\Delta_{\mathbf{k}}^-) = -\text{sgn}(\Delta_{\tilde{\mathbf{k}}}^-)$. The latter condition corresponds to the topologically protected zero-energy surface bands found in Ref. 13, which occur within a finite region of the surface Brillouin zone bounded by the projected nodes of the bulk gap. It is interesting that this condition is quite similar to the one for zero-energy states at surfaces of unconventional *centrosymmetric* superconductors, i.e., the sign of the gap must reverse between \mathbf{k} and $\tilde{\mathbf{k}}$. It is therefore somewhat surprising that the relative sign between the gaps on *different* helicity bands at these wave vectors is irrelevant, despite the

mixing of the helicity components in the edge-state wave function.

In Figs. 1(b), 1(d), and 1(f), we plot the dispersion of the bound states appearing at the (111) surface of an NCS with point group C_{4v} , O , and T_d , respectively. For all three point groups, we find singly degenerate zero-energy surface bands for $0 < q < 1$, i.e., there are two-dimensional regions in the surface Brillouin zone where the energy of the bound states vanishes [black regions in Figs. 1(b), 1(d), and 1(f)]. As can be seen by comparison with Figs. 1(a), 1(c), and 1(e), these occur where the sign of $\Delta_{\mathbf{k}}^-$ on the forward-facing half of the Fermi surface is different to that on the backward-facing half. This is a manifestation of the bulk-boundary correspondence found in Ref. 13, which relates the topologically stable nodal lines of the bulk gap to the zero-energy surface bands. A quantized topological invariant is associated with the line nodes, which protects them and hence also the zero-energy surface bands from sufficiently small symmetry-preserving perturbations. Large perturbations, which remove the nodal rings (e.g., increasing the singlet-to-triplet ratio q past 1), therefore also destroy the associated zero-energy surface bands.

The zero-energy surface bands are in general accompanied by dispersing modes [colored regions in Figs. 1(b), 1(d), and 1(f)], which occur in regions of the surface Brillouin zone where $\text{sgn}(\Delta_{\mathbf{k}}^-) = \text{sgn}(\Delta_{\mathbf{k}}^+) = -1$. The coexistence of dispersive and nondispersive surface states gives rise to intricate bound-state spectra. In the case of the C_{4v} point group [Fig. 1(a)], the linearly dispersing states at sufficiently small $|k_{2,\parallel}|$ arise from the same mechanism as the states found along the (100) direction in Ref. 21. Note the line of zero-energy states at $k_{1,\parallel} = 0$ connecting the two flat bands.

IV. TUNNELING CONDUCTANCE

Although the surface bound states do not form at an interface with a normal metal, for a low-transparency barrier between a metal and an NCS, the physical mechanism discussed above leads to the formation of interface-resonance states. For a surface that displays zero-energy bands, it is well known that the corresponding tunnel junction will show a sharp ZBCP in the low-temperature tunneling conductance. As in the case of the d -wave gap in the high- T_c cuprates,^{8,32} a direction-dependent ZBCP in an NCS due to the topologically protected zero-energy surface bands would be a key experimental signature of the pairing state.

The zero-temperature charge conductance $\sigma_S(\text{eV})$ for tunneling into the NCS is a generalization of the usual Blonder-Tinkham-Klapwijk formula^{20,21,25,33}

$$\sigma_S(\text{eV}) = \sum_{\mathbf{k}_{\parallel}} \left\{ 1 + \frac{1}{2} \sum_{\sigma, \sigma'} [|a_{\mathbf{k}_{\parallel}}^{\sigma, \sigma'}|^2 - |b_{\mathbf{k}_{\parallel}}^{\sigma, \sigma'}|^2] \right\}, \quad (6)$$

where $a_{\mathbf{k}_{\parallel}}^{\sigma, \sigma'}$ and $b_{\mathbf{k}_{\parallel}}^{\sigma, \sigma'}$ are the Andreev and normal reflection for electron injection into the NCS, respectively. These coefficients are determined by solving the BdG equation for the junction at energy $E = \text{eV}$, with the wave-function ansatz $\Psi_{\sigma}(\mathbf{k}_{\parallel}, \mathbf{r}) = \Theta(-r_{\perp})\psi_{\mathbf{k}_{\parallel}, \sigma}^<(\mathbf{r}) + \Theta(r_{\perp})\psi_{\mathbf{k}_{\parallel}, \sigma}^>(\mathbf{r})$, where

$$\begin{aligned} \psi_{\mathbf{k}_{\parallel}, \sigma}^<(\mathbf{r}) &= \psi_{e, \sigma} e^{i\mathbf{k}\cdot\mathbf{r}} + \sum_{\sigma'=\uparrow, \downarrow} [a_{\mathbf{k}_{\parallel}}^{\sigma, \sigma'} \psi_{h, \sigma'} e^{i\mathbf{k}\cdot\mathbf{r}} + b_{\mathbf{k}_{\parallel}}^{\sigma, \sigma'} \psi_{e, \sigma'} e^{i\tilde{\mathbf{k}}\cdot\mathbf{r}}], \\ \psi_{\mathbf{k}_{\parallel}, \sigma}^>(\mathbf{r}) &= \sum_{n=\pm} [c_{\mathbf{k}_{\parallel}}^{\sigma, n} \psi_n(\mathbf{k}) e^{i\mathbf{k}\cdot\mathbf{r}} + d_{\mathbf{k}_{\parallel}}^{\sigma, n} \psi_n(\tilde{\mathbf{k}}) e^{i\tilde{\mathbf{k}}\cdot\mathbf{r}}]. \end{aligned} \quad (7)$$

$\psi_{e, \sigma} = \frac{1}{2}(1 + \sigma, 1 - \sigma, 0, 0)^T$ and $\psi_{h, \sigma} = \frac{1}{2}(0, 0, 1 + \sigma, 1 - \sigma)^T$ are the electron and hole spinors in the normal metal, respectively. We adopt the assumption that the bias energy is small compared to the Fermi energy so that the wave vectors in Eq. (7) are well approximated to have magnitude k_F .^{20,23} The insulating barrier at $r_{\perp} = 0$ is modeled as a δ function of height U . The coefficients in Eq. (7) are then chosen such that Ψ_{σ} is continuous at the interface, i.e., $\Psi_{\sigma}(\mathbf{k}_{\parallel}, \mathbf{r})|_{r_{\perp}=0^-} = \Psi_{\sigma}(\mathbf{k}_{\parallel}, \mathbf{r})|_{r_{\perp}=0^+}$, while the derivative obeys

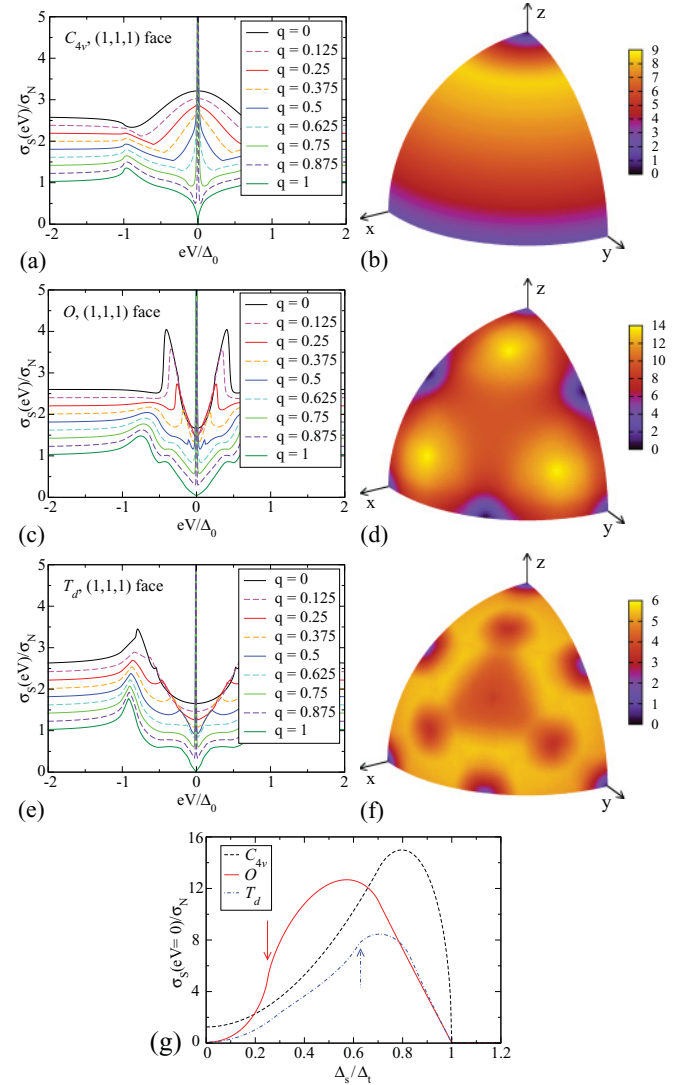


FIG. 2. (Color online) Panels (a), (c) and (e): Normalized conductance spectra at the (111) face for an NCS with point group (a) C_{4v} , (c) O , and (e) T_d and various values of $0 \leq q = \Delta_s/\Delta_t \leq 1$. In all panels we take $Z = 3$ and $T = 0$ K. Curves are vertically shifted by multiples of 0.2. Panels (b), (d) and (f): ZBCP as a function of surface orientation for an NCS with point group (b) C_{4v} with $q = 0.5$, (d) O with $q = 0.35$, and (f) T_d with $q = 0.4$. The color at each point on the sphere indicates the height of the ZBCP for the corresponding normal vector. Panel (g): Variation of ZBCP height at the (111) face as a function of q .

$\partial_{r_{\perp}} \Psi_{\sigma}(\mathbf{k}_{\parallel}, \mathbf{r})|_{r_{\perp}=0^{+}} - \partial_{r_{\perp}} \Psi_{\sigma}(\mathbf{k}_{\parallel}, \mathbf{r})|_{r_{\perp}=0^{-}} = 2Z\Psi_{\sigma}(\mathbf{k}_{\parallel}, \mathbf{r})|_{r_{\perp}=0}$, where $Z = mU/\hbar^2$ with m is the effective mass, assumed the same in the NCS and the metal.

In Figs. 2(a), 2(c), and 2(e), we show the conductance spectra at the (111) face for the C_{4v} , O , and T_d point groups, respectively. The spectra are normalized by the normal-state conductance $\sigma_N = \sum_{\mathbf{k}_{\parallel}} |\mathbf{k}_{\parallel}|^2 / (Z^2 + |\mathbf{k}_{\parallel}|^2)$. For $0 < q < 1$, we find a sharp ZBCP, signaling the existence of the zero-energy surface bands. For the most part, this peak is well separated from the contributions of dispersing states or the edges of the bulk gap. A notable exception is the C_{4v} case [Fig. 2(a)], where, for small q , we find the ZBCP superimposed on a wide domelike feature due to the dispersing surface modes.^{21,25} As shown in Fig. 2(g), the ZBCP vanishes as $q \rightarrow 1$ and is absent for $q > 1$, consistent with the topologically trivial gapped state that forms when the singlet pairing dominates. We note that, in the case of the O and T_d point groups, the ZBCP height shows kinks as a function of q , marked by the arrows in Fig. 2(g). At these values of q , there is a Lifshitz-type transition in the BdG spectrum at which the nodal rings touch each other and then reconnect.

Finally, we consider the direction dependence of the ZBCP [Figs. 2(b), 2(d), and 2(f)]. The strong variation in the conductance with the surface orientation reflects the changing projection of the bulk nodal lines onto the surface Brillouin zone. Note that the ZBCP is absent along the crystal axes for all point groups. This can be exploited as a probe of the pairing state in an NCS: For example, the observation of a ZBCP along the (111) direction, but its absence along the (100) direction, would lend strong support to a model of an NCS pairing state with a dominant triplet component. Since the zero-energy surface bands responsible for the ZBCP are topologically protected, we expect this to be a particularly robust test of the superconducting state.

V. CONCLUSIONS

In this Rapid Communication, we have used quasiclassical scattering theory to study the appearance of topologically protected zero-energy bands at the surface of NCS for three experimentally relevant choices of the point group. We have derived a general condition for the existence of these states, which is consistent with the bulk-boundary correspondence found in Ref. 13. The surface-bound-state spectrum has been computed and shown to allow the coexistence of zero-energy flat bands with dispersing states. We have also calculated the tunneling conductance, where the presence of these zero-energy states manifests itself as a ZBCP. The ZBCP displays a strong dependence on the surface orientation and, in particular, vanishes along the crystal axes. Not only can this dependence be exploited as a test of the orbital and spin pairing symmetries in these materials, but the ZBCP also directly evidences the topologically protected zero-energy surface bands. Our paper therefore makes the case for NCS as a model gapless topological superconducting system, in analogy to the role of Bi_2Se_3 , Bi_2Te_3 , and related semiconductors as the reference systems for spin-orbit-induced topological insulators.³

Prospects for further work are promising. For example, the large degeneracy of the zero-energy surface bands may be expected to lead to instabilities toward symmetry-broken states in the presence of interactions. The possible coexistence of time-reversal-symmetry-breaking and time-reversal-symmetry-preserving order parameters near the surface of an NCS is particularly tantalizing.

ACKNOWLEDGMENT

The authors thank A. Avella, S. Ryu, and M. Sigrist for useful discussions.

*brydon@theory.phy.tu-dresden.de

†a.schnyder@fkf.mpg.de

¹M. Z. Hasan and C. L. Kane, *Rev. Mod. Phys.* **82**, 3045 (2010).

²X.-L. Qi and S.-C. Zhang, e-print [arXiv:1008.2026v1](https://arxiv.org/abs/1008.2026v1).

³M. Z. Hasan and J. E. Moore, *Ann. Rev. Cond. Matt. Phys.* **2**, 55 (2011).

⁴S. Ryu *et al.*, *New J. Phys.* **12**, 065010 (2010).

⁵K. Nakada *et al.*, *Phys. Rev. B* **54**, 17954 (1996).

⁶M. Fujita *et al.*, *J. Phys. Soc. Jpn.* **65**, 1920 (1996).

⁷C.-R. Hu, *Phys. Rev. Lett.* **72**, 1526 (1994).

⁸S. Kashiwaya and Y. Tanaka, *Rep. Prog. Phys.* **63**, 1641 (2000).

⁹G. E. Volovik, *Pis'ma ZhETF* **93**, 69 (2011) [*JETP Lett.* **93**, 69 (2011)].

¹⁰T. T. Heikkilä and G. E. Volovik, *Pis'ma ZhETF* **93**, 63 (2011) [*JETP Lett.* **93**, 63 (2011)]. T. T. Heikkilä, N. B. Kopnin, and G. E. Volovik, e-print [arXiv:1012.0905v4](https://arxiv.org/abs/1012.0905v4).

¹¹M. Sato, *Phys. Rev. B* **73**, 214502 (2006).

¹²B. Béri, *Phys. Rev. B* **81**, 134515 (2010).

¹³A. P. Schnyder and S. Ryu, e-print [arXiv:1011.1438](https://arxiv.org/abs/1011.1438).

¹⁴K. Togano *et al.*, *Phys. Rev. Lett.* **93**, 247004 (2004).

¹⁵P. Badica, T. Kondo, and K. Togano, *J. Phys. Soc. Jpn.* **74**, 1014 (2005).

¹⁶G. Amano *et al.*, *J. Phys. Soc. Jpn.* **73**, 530 (2004).

¹⁷E. Bauer *et al.*, *Phys. Rev. Lett.* **92**, 027003 (2004).

¹⁸N. Kimura *et al.*, *Phys. Rev. Lett.* **95**, 247004 (2005).

¹⁹I. Sugitani *et al.*, *J. Phys. Soc. Jpn.* **75**, 043703 (2006).

²⁰T. Yokoyama, Y. Tanaka, and J. Inoue, *Phys. Rev. B* **72**, 220504(R) (2005).

²¹C. Iniotakis *et al.*, *Phys. Rev. B* **76**, 012501 (2007).

²²A. B. Vorontsov, I. Vekhter, and M. Eschrig, *Phys. Rev. Lett.* **101**, 127003 (2008); A. Vorontsov, I. Vekhter, and M. Eschrig, *Phys. B (Amsterdam)* **403**, 1095 (2008).

²³Y. Tanaka *et al.*, *Phys. Rev. B* **79**, 060505(R) (2009).

²⁴Y. Tanaka *et al.*, *Phys. Rev. Lett.* **105**, 097002 (2010).

²⁵M. Eschrig, C. Iniotakis, and Y. Tanaka, e-print [arXiv:1001.2486v1](https://arxiv.org/abs/1001.2486v1).

²⁶P. A. Frigeri *et al.*, *Phys. Rev. Lett.* **92**, 097001 (2004).

²⁷The relative signs of Δ_s and Δ_t determine the presence of nodes in either the positive or negative helicity gaps. In the following, we regard the SO splitting of the bands as insignificant, allowing us to fix the signs without loss of generality.

²⁸M. Sato and S. Fujimoto, *Phys. Rev. Lett.* **105**, 217001 (2010).

²⁹K. Yada *et al.*, *Phys. Rev. B* **83**, 064505 (2011).

³⁰M. Sato *et al.*, *Phys. Rev. B* **83**, 224511 (2011).

³¹K. V. Samokhin, *Ann. Phys. (NY)* **324**, 2385 (2009).

³²J. Y. T. Wei *et al.*, *Phys. Rev. Lett.* **81**, 2542 (1998).

³³G. E. Blonder, M. Tinkham, and T. M. Klapwijk, *Phys. Rev. B* **25**, 4515 (1982).